Eur. Phys. J. C 44, 559–566 (2005)
Digital Object Identifier (DOI) 10.1140/epjc/s2005-02393-7

THE EUROPEAN PHYSICAL JOURNAL C

Higgs boson production at hadron colliders in the k_{T}-factorization approach

A.V. Lipatov[a], N.P. Zotov

D.V. Skobeltsyn Institute of Nuclear Physics, M.V. Lomonosov Moscow State University, 119992 Moscow, Russia

Received: 26 January 2005 / Revised version: 8 July 2005 /
Published online: 6 October 2005 –

Abstract. We consider the Higgs boson production at high energy hadron colliders in the framework of the k_{T}-factorization approach. The attention is focused on the dominant gluon–gluon fusion subprocess. We calculate the total cross section and transverse momentum distributions of the inclusive Higgs production using unintegrated gluon distributions in a proton obtained from the full CCFM evolution equation. We show that k_{T}-factorization gives a possibility to investigate the associated Higgs boson and jets production. We calculate the transverse momentum distributions and study the Higgs–jet and jet–jet azimuthal correlations in the Higgs + one or two jet production processes. We demonstrate the importance of the higher-order corrections within the k_{T}-factorization approach. These corrections should be developed and taken into account in the future applications.

1 Introduction

It is well known that electroweak symmetry breaking in the standard model of elementary particle interactions is achieved via the Higgs mechanism. In the minimal model there is a single complex Higgs doublet, where the Higgs boson H is the physical neutral Higgs scalar which is the only remaining part of this doublet after spontaneous symmetry breaking. In non-minimal models there are additional charged and neutral scalar Higgs particles. The search for the Higgs boson takes important part at the Fermilab Tevatron experiments and will be one of the main fields of study at the CERN LHC collider [1]. The experimental detection of the H will be great triumph of the standard model of electroweak interactions and will mark a new stage in high energy physics.

At LHC conditions, the gluon–gluon fusion $gg \to H$ is the dominant inclusive Higgs production mechanism [2,3]. In this process, the Higgs production occurs via triangle heavy (top) quark loop. Gluon fusion and weak boson fusion ($qq \to qqH$ subprocess via t-channel exchange of a W or Z bosons) are also expected to be the dominant sources of semi-inclusive Higgs production (in association with one or two hadronic jets) [4]. Detailed theoretical studies of such processes are necessary, in particular, to determine an optimal set of cuts on the final state particles.

It is obvious that the gluon–gluon fusion contribution to the Higgs production at LHC is strongly dependent on the gluon density $xG(x,\mu^2)$ in a proton. Usually the gluon density is described by the Dokshitzer–Gribov–Lipatov–Altarelli–Parisi (DGLAP) evolution equation [5] where large logarithmic terms proportional to $\ln \mu^2$ are taken into account. The cross sections can be rewritten in terms of hard matrix elements convoluted with gluon density functions. In this way the dominant contributions come from diagrams where the parton emissions in the initial state are strongly ordered in virtuality. This is called collinear factorization, as the strong ordering means that the virtuality of the parton entering the hard scattering matrix elements can be neglected compared to the large scale μ^2. However, at the LHC energies, typical values of the incident gluon momentum fractions $x \sim m_H/\sqrt{s} \sim 0.008$ (for Higgs boson mass $m_H = 120\,\mathrm{GeV}$) are small, and other large logarithmic terms proportional to $\ln 1/x$ become important. These contributions can be taken into account using the Balitsky–Fadin–Kuraev–Lipatov (BFKL) evolution equation [6]. Just as for DGLAP, in this way it is possible to factorize an observable into a convolution of process-dependent hard matrix elements with universal gluon distributions. But as the virtualities (and transverse momenta) of the propagating gluons are no longer ordered, the matrix elements have to be taken off-shell and the convolution made also over transverse momentum $\mathbf{k}_{\mathrm{T}}$ with the unintegrated (k_{T}-dependent) gluon distribution $\mathcal{F}(x,\mathbf{k}_{\mathrm{T}}^2)$. The unintegrated gluon distribution $\mathcal{F}(x,\mathbf{k}_{\mathrm{T}}^2)$ determines the probability to find a gluon carrying the longitudinal momentum fraction x and the transverse momentum $\mathbf{k}_{\mathrm{T}}$. This generalized factorization is called k_{T}-factorization [7–10]. It is expected that BFKL evolution gives the theoretically correct description at assymptotically large energies (i.e. very small x). At the same time another approach, valid for both small and large x, has been developed by Ciafaloni, Catani, Fiorani and Marchesini, and is known as the CCFM model [11]. It introduces angular ordering

[a] e-mail: artem.lipatov@mail.ru

of emissions to correctly treat gluon coherence effects. In the limit of asymptotic energies it is almost equivalent to BFKL [12–14], but also similar to the DGLAP evolution for large x and high μ^2. The resulting unintegrated gluon distribution depends on two scales, the additional scale $\bar{q}^2$ is a variable related to the maximum angle allowed in the emission and plays the role of the evolution scale μ^2 in the collinear parton densities. The following classification scheme [15] is used: the $\mathcal{F}(x, \mathbf{k}_T^2)$ denote pure BFKL-type unintegrated gluon distributions and $\mathcal{A}(x, \mathbf{k}_T^2, \mu^2)$ stands for any other type having two scale involved. In this paper we will apply the CCFM gluon evolution to study the inclusive and semi-inclusive Higgs production at LHC conditions.

In the collinear factorization, the calculation of such processes is quite complicated even at lowest order because of the heavy quark loops contribution. For example, in Higgs + one jet production, triangle and box loops occur, and in Higgs + two jet production the pentagon loops occur [16]. However, the calculations of the Higgs production rates can be simplified in the limit of large top-quark mass $m_t \to \infty$ [17]. In this approximation the coupling of the gluons to the Higgs via a top-quark loop can be replaced by an effective coupling. Thus it reduces the number of loops in a given diagram by one. The large m_t approximation is valid to an accuracy of $\sim 5\%$ in the intermediate Higgs mass range $m_H < 2m_t$, as long as the transverse momenta of the Higgs or final jets are smaller than the ones of the top-quark mass ($p_T < m_t$) [16]. Within this approach, the total cross section for $gg \to H + X$ is known to next-to-next-to-leading order (NNLO) accuracy [18]. Higher-order QCD corrections to inclusive Higgs production were found to be large: their effect increases the leading-order cross section by about 80–100% [19, 20].

A particularly interesting quantity is the transverse momentum distribution of the produced Higgs boson. The precise theoretical prediction of the $\mathrm{d}\sigma/\mathrm{d}p_T$ at the LHC is important for quantitative evaluation of the required measurement accuracies and detector performance. It is well known that the fixed-order perturbative QCD is applicable when the Higgs transverse momentum is comparable to the m_H. However, the main part of the events is expected in the small-p_T region ($p_T \ll m_H$), where the coefficients of the perturbative series in α_s are enhanced by powers of large logarithmic terms proportional to $\ln m_H^2/p_T^2$. Therefore reliable predictions at small p_T can only be obtained if these terms will be resummed to all orders. Such a procedure is called soft-gluon resummation [21–23] and has been performed in collinear calculations at leading logarithmic (LL), next-to-leading logarithmic (NLL) [24] and next-to-next-to-leading logarithmic (NNLL) [25] levels. Recently it was shown [26] that in the framework of the k_T-factorization approach the soft-gluon resummation formulas are the result of the approximate treatment of the solutions of the CCFM evolution equation (in the b-representation).

There are several additional motivations for our study of the Higgs production in the k_T-factorization approach. First of all, in the standard collinear approach, when the transverse momentum of the initial gluons is neglected, the transerse momentum of the final Higgs boson in $gg \to H$ subprocess is zero. Therefore it is necessary to include initial-state QCD radiation to generate the p_T distributions. It is well known at present that the k_T-factorization naturally includes a large part of the high-order perturbative QCD corrections [27]. This fact is illustrated more detailed in Fig. 1, which is a schematical representation of a typical Higgs + jet production process. Figure 1a shows the fixed-order perturbative QCD picture where the upper part of the diagram (above the dash-dotted line) corresponds to the $gg \to gH$ subprocess, and the lower part describes the gluon evolution in a proton. As the incoming gluons are assumed to have zero transverse momentum, the transverse momentum distributions of the produced Higgs and jet are totally determined by the properties of the $\mathcal{O}(\alpha_s^3)$ matrix element. In the k_T-factorization approach (Fig. 1b), the underlying partonic subprocess is $gg \to H$, which is formally of order $\mathcal{O}(\alpha_s^2)$. Some extra powers of α_s are hidden in the gluon evolution represented by the part of the diagram shown below the dash-dotted line. In contrast with the collinear approximation, the k_T-factorization takes into account the gluon transverse motion. Since the upper gluon in the parton ladder is not included in the hard interaction, its transverse momentum is now determined by the properties of the evolution equation only. It means that in the k_T-factorization approach the study of transverse momenta distributions in the Higgs production via gluon–gluon fusion will be a direct probe of the unintegrated gluon distributions in a proton. In this case the transverse momentum of the produced Higgs should be equal to the sum of the transverse momenta of the initial gluons. Therefore future experimental studies at LHC can be used as a further test of the non-collinear parton evolution.

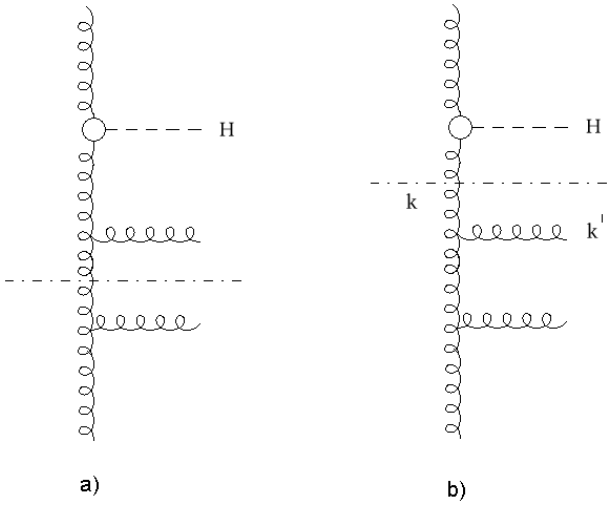

Fig. 1. The typical Feynman diagram contributing to the Higgs boson production in the collinear **a** and k_T-factorization **b** approaches

In the previous studies [26, 28, 29] the k_T-factorization formalism was applied to calculate the transverse momentum distribution of the inclusive Higgs production. The simplified solution of the CCFM equation in single loop approximation [30] (when small-x effects can be neglected)

were used in [26]. In such an approximation the CCFM evolution is reduced to the DGLAP one with the difference that the single loop evolution takes the gluon transverse momentum $k_{\rm T}$ into account. Another simplified solution of the CCFM equation was proposed in [31], where the transverse momenta of the incoming gluons are generated in the last evolution step (Kimber–Martin–Ryskin prescription). The calculations [26,29] were done using the on-mass shell (independent from the gluon $k_{\rm T}$) matrix element of the $gg \to H$ subprocess and rather similar results have been obtained. In [28] in the framework of the MC generator CASCADE [32] the off-mass-shell matrix element obtained by Hautmann [33] has been used with full CCFM evolution.

In present paper we investigate Higgs production at hadron colliders using the full CCFM-evolved unintegrated gluon densities [28]. We obtain the obvious expression for the $g^*g^* \to H$ off-mass-shell matrix element in the large m_t limit apart from [33]. After that, we calculate the total cross section and transverse momentum distribution of the inclusive Higgs production at Tevatron and LHC. To illustrate the fact that in the $k_{\rm T}$-factorization approach the main features of collinear higher-order pQCD corrections are taken into account effectively, we give theoretical predictions for the Higgs + one jet and Higgs + two jet production processes using some physically motivated approximation.

In Sect. 2 we recall the basic formulas of the $k_{\rm T}$-factorization formalism with a brief review of calculation steps. In Sect. 3 we present the numerical results of our calculations and a discussion. Finally, in Sect. 4, we give a summary of our results.

2 Basic formulas

We start from the effective Lagrangian for the Higgs boson coupling to gluons [16]:

$$\mathcal{L}_{\rm eff} = \frac{\alpha_{\rm s}}{12\pi}\left(G_{\rm F}\sqrt{2}\right)^{1/2} G^a_{\mu\nu}G^{a\,\mu\nu}H, \tag{1}$$

where $G_{\rm F}$ is the Fermi coupling constant, $G^a_{\mu\nu}$ is the gluon field strength tensor and H is the Higgs field. The triangle vertex $T^{\mu\nu}(k_1,k_2)$ for two off-shell gluons having four-momenta k_1 and k_2 and color indexes a and b respectively, can be obtained easily from the Lagrangian (1):

$$T^{\mu\nu}(k_1,k_2) = {\rm i}\delta^{ab}\frac{\alpha_{\rm s}}{3\pi}\left(G_{\rm F}\sqrt{2}\right)^{1/2}\left[k_2^\mu k_1^\nu - (k_1\cdot k_2)g^{\mu\nu}\right]. \tag{2}$$

To calculate the squared off-mass-shell matrix element for the $g^*g^* \to H$ subprocess it is necessary to take into account the non-zero virtualities of the initial gluons $k_1^2 = -\mathbf{k}_{1\rm T}^2 \neq 0$, $k_2^2 = -\mathbf{k}_{2\rm T}^2 \neq 0$. We have obtained

$$|\bar{\mathcal{M}}|^2(g^*g^* \to H) = \frac{\alpha_{\rm s}^2(\mu^2)}{576\pi^2}G_{\rm F}\sqrt{2} \times \left[m_H^2 + \mathbf{k}_{1\rm T}^2 + \mathbf{k}_{2\rm T}^2 + 2|\mathbf{k}_{1\rm T}||\mathbf{k}_{2\rm T}|\cos\phi\right]^2\cos^2\phi, \tag{3}$$

where ϕ is the azimuthal angle between transverse momenta $\mathbf{k}_{1\rm T}$ and $\mathbf{k}_{2\rm T}$, the transverse momentum of the produced Higgs boson is $\mathbf{p}_{\rm T} = \mathbf{k}_{1\rm T} + \mathbf{k}_{2\rm T}$ and the virtual gluon polarization tensor has been taken in the form [7,8]

$$\sum \epsilon^\mu \epsilon^{*\,\nu} = \frac{k_{\rm T}^\mu k_{\rm T}^\nu}{\mathbf{k}_{\rm T}^2}. \tag{4}$$

The cross section of the inclusive Higgs production $p\bar{p} \to H + X$ in the $k_{\rm T}$-factorization approach can be written as

$$\mathrm{d}\sigma(p\bar{p} \to H + X) = \int \frac{\mathrm{d}x_1}{x_1}\mathcal{A}(x_1,\mathbf{k}_{1\rm T}^2,\mu^2)\mathrm{d}\mathbf{k}_{1\rm T}^2\frac{\mathrm{d}\phi_1}{2\pi} \times \int \frac{\mathrm{d}x_2}{x_2}\mathcal{A}(x_2,\mathbf{k}_{2\rm T}^2,\mu^2)\mathrm{d}\mathbf{k}_{2\rm T}^2\frac{\mathrm{d}\phi_2}{2\pi}\mathrm{d}\hat{\sigma}(g^*g^* \to H), \tag{5}$$

where $\hat{\sigma}(g^*g^* \to H)$ is the Higgs production cross section with off-mass-shell gluons, x_1 and x_2 are the longitudinal momentum fractions, and $\mathcal{A}(x,\mathbf{k}_{\rm T}^2,\mu^2)$ is the unintegrated gluon distribution in a proton. Let $s = (p_1+p_2)^2$ and p_1 and p_2 be the four-vectors of the incoming protons. Then the differential cross section reads[1]

$$\frac{\mathrm{d}\sigma(p\bar{p} \to H + X)}{\mathrm{d}y_H} = \int \frac{\alpha_{\rm s}^2(\mu^2)}{288\pi}\frac{G_{\rm F}\sqrt{2}}{x_1x_2m_H^2s}\left[m_H^2 + \mathbf{p}_{\rm T}^2\right]^2\cos^2\phi_2 \times \mathcal{A}(x_1,\mathbf{k}_{1\rm T}^2,\mu^2)\mathcal{A}(x_2,\mathbf{k}_{2\rm T}^2,\mu^2)\mathrm{d}\mathbf{k}_{1\rm T}^2\mathrm{d}\mathbf{k}_{2\rm T}^2\frac{\mathrm{d}\phi_2}{2\pi}, \tag{6}$$

where y_H is the Higgs rapidity in the proton–proton CM frame. The longitudinal momentum fractions x_1 and x_2 are given by

$$x_1 = \sqrt{\frac{m_H^2 + \mathbf{p}_{\rm T}^2}{s}}\exp(y_H), \qquad x_2 = \sqrt{\frac{m_H^2 + \mathbf{p}_{\rm T}^2}{s}}\exp(-y_H). \tag{7}$$

If we average the expression (6) over transverse momenta $\mathbf{k}_{1\rm T}$ and $\mathbf{k}_{2\rm T}$ and take the limit $\mathbf{k}_{1\rm T}^2 \to 0$, $\mathbf{k}_{2\rm T}^2 \to 0$, we obtain the well-established expression [2] for the Higgs production cross section in leading-order perturbative QCD:

$$\mathrm{d}\sigma(p\bar{p} \to H + X) = \frac{\alpha_{\rm s}^2(\mu^2)}{576\pi}G_{\rm F}\sqrt{2}\frac{m_H^2}{x_1x_2s}x_1\mathcal{G}(x_1,\mu^2)x_2\mathcal{G}(x_2,\mu^2)\mathrm{d}y_H, \tag{8}$$

where $x\mathcal{G}(x,\mu^2)$ is the usual (collinear) gluon density which is related with the unintegrated gluon distribution $\mathcal{A}(x,\mathbf{k}_{\rm T}^2,\mu^2)$ by

$$x\mathcal{G}(x,\mu^2) \sim \int \mathcal{A}(x,\mathbf{k}_{\rm T}^2,\mu^2)\mathrm{d}\mathbf{k}_{\rm T}^2. \tag{9}$$

[1] We would like to remark that the expression (6) differs inessentially from the one obtained in [33].

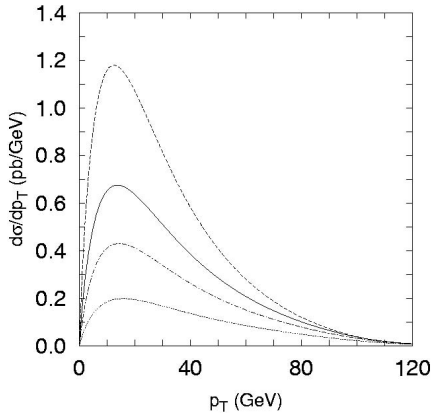

Fig. 2. Differential cross section $\mathrm{d}\sigma/\mathrm{d}p_{\rm T}$ for inclusive Higgs boson production at $\sqrt{s} = 14\,\mathrm{TeV}$. The solid, dashed, dash-dotted and dotted lines correspond to $m_H = 125\,\mathrm{GeV}$, $m_H = 100\,\mathrm{GeV}$, $m_H = 150\,\mathrm{GeV}$ and $m_H = 200\,\mathrm{GeV}$, respectively

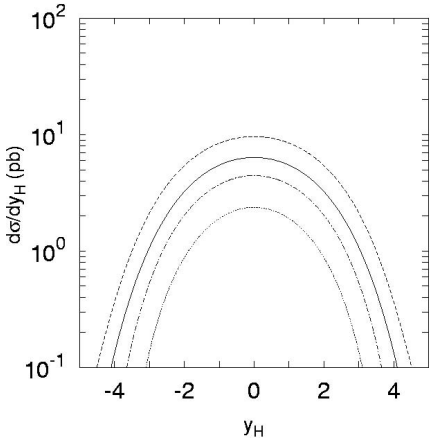

Fig. 3. Differential cross section $\mathrm{d}\sigma/\mathrm{d}y_H$ for inclusive Higgs boson production at $\sqrt{s} = 14\,\mathrm{TeV}$. All curves are the same as in Fig. 2

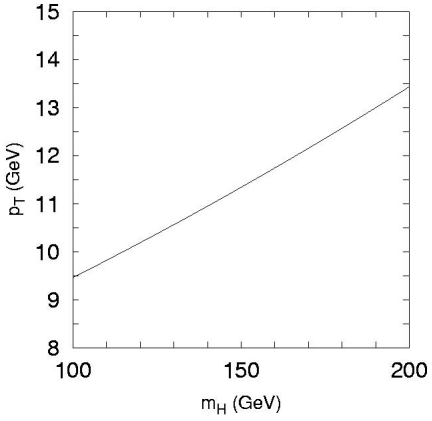

Fig. 4. Location of the peak of the transverse momentum distributions for inclusive Higgs boson production as a function of Higgs mass at $\sqrt{s} = 14\,\mathrm{TeV}$

Here the sign $\sim$ indicates, that there is no strict equality between the left and the right parts of (9)[2].

The multidimensional integration in the expression (6) has been performed by means of the Monte Carlo technique, using the routine VEGAS [35]. The full C++ code is available from the authors on request[3].

3 Numerical results and discussion

3.1 Inclusive Higgs production

We now are in a position to present our numerical results. First we describe our theoretical input and the kinematical conditions. Besides the Higgs mass m_H, the cross section (6) depends on the unintegrated gluon distribution $\mathcal{A}(x, \mathbf{k}_{\rm T}^2, \mu^2)$ and the energy scale μ. The new fits of the unintegrated gluon density (J2003 set 1–3) have been recently presented [28]. The full CCFM equation in a proton was solved numerically using a Monte Carlo method. The input parameters were fitted to describe the proton structure function $F_2(x, Q^2)$. Since these gluon densities reproduce well the forward jet production at HERA, charm and bottom production data at Tevatron [28] and charm and J/ψ production at LEP2 energies [36], we use it in our calculations. As is often done for Higgs production, we choose the renormalization and factorization scales to be $\mu = \xi m_H$, and vary the scale parameter ξ between 1/2 and 2 about the default value $\xi = 1$. Also we use the LO formula for the strong coupling constant $\alpha_{\rm s}(\mu^2)$ with $n_f = 4$ active quark flavors and $\Lambda_{\rm QCD} = 200\,\mathrm{MeV}$, such that $\alpha_{\rm s}(M_Z^2) = 0.1232$.

In Figs. 2 and 3 we display our prediction for the transverse momentum and rapidity distributions of the inclusive Higgs production at the LHC ($\sqrt{s} = 14\,\mathrm{TeV}$). The calculations were done for four choices of the Higgs boson mass under interest in the standard model with default scale $\mu^2 = m_H^2$. The solid, dashed, dash-dotted and dotted lines correspond to $m_H = 125\,\mathrm{GeV}$, $m_H = 100\,\mathrm{GeV}$, $m_H = 150\,\mathrm{GeV}$ (where the WW decay channel is dominant) and $m_H = 200\,\mathrm{GeV}$ (above the WW and ZZ decay tresholds), respectively. One can see that mass effects are present only at low $p_{\rm T} < m_H$, whereas all curves practically coincide at large transverse momenta. We note that our predictions which correspond to the Higgs mass $m_H = 125\,\mathrm{GeV}$ slightly underestimate the results obtained in the combined fixed-order + resummed approach [37]. In this approach fixed-order predictions (at LO or NLO level) and resummed ones (at NLL or NNLL level, respectively) have to be consistently matched at moderate $p_{\rm T}$. The NNLL + NLO results [25] are smaller than NLL + LO ones [24] by about 20% at low transverse momenta. We see that our predictions lie below NNLL + NLO calculations by about 15% in this kinematical region. Using the doubly unintegrated gluon distributions results in a more flat behavior of the $p_{\rm T}$-distribution [29] in comparison with both our and NNLL + NLO predictions.

We note also that the peak in the transverse momentum distribution occurs at a smaller value of $p_{\rm T}$ compared to the NNLL + NLO calculations. The location of this peak as a function of the Higgs boson mass is shown in Fig. 4. We find that at $m_H = 125\,\mathrm{GeV}$ the peak occurs at $p_{\rm T} \sim 10\,\mathrm{GeV}$, whereas NNLL + NLO line peaks at $p_{\rm T} \sim 15\,\mathrm{GeV}$ [37]. A similar effect has been obtained [29] when doubly unintegrated gluon distributions were used.

The total cross sections of the inclusive Higgs production at Tevatron ($\sqrt{s} = 1.96\,\mathrm{TeV}$) and LHC conditions as a function of the Higgs mass are plotted in Figs. 5 and 6 in the mass range $m_H = 100$–$200\,\mathrm{GeV}$. The solid lines are obtained by fixing both the factorization and renormalization scales at the default value $\mu = m_H$ using J2003 set 1 unintegrated gluon density. Additionally, in order to in-

[2] See [15, 34] for more details.

[3] e-mail: lipatov@theory.sinp.msu.ru

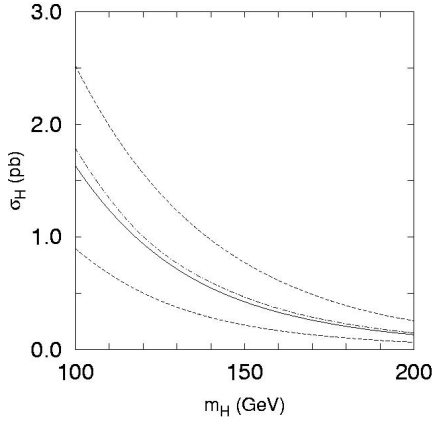

Fig. 5. Total cross section of inclusive Higgs boson production as a function of Higgs mass at $\sqrt{s} = 1.96\,\text{TeV}$. The solid and both dashed lines are obtained using J2003 set 1 unintegrated gluon density. The solid line corresponds to the default scale $\mu = m_H$, whereas upper and lower dashed lines correspond to the $\mu = m_H/2$ and $\mu = 2m_H$ scales, respectively. The dash-dotted line is obtained using J2003 set 3 unintegrated gluon with the default scale $\mu = m_H$

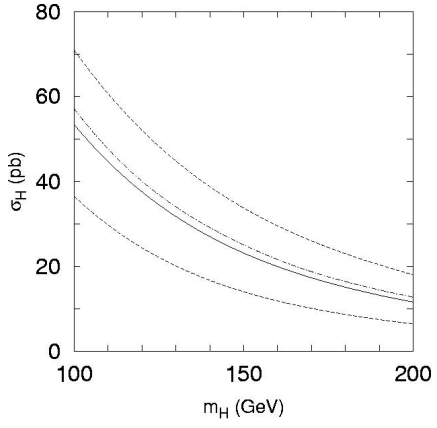

Fig. 6. Total cross section of inclusive Higgs boson production as a function of Higgs mass at $\sqrt{s} = 14\,\text{TeV}$. All curves are the same as in Fig. 5

vestigate the sensitivity of our results to the non-collinear evolution details, we have repeated our calculation using the J2003 set 3 unintegrated gluon distribution [28] at the default scale (dash-dotted lines in Figs. 5 and 6). One can see that the difference between the J2003 set 1 and set 3 predictions is rather small[4]. Then in order to estimate the theoretical uncertainties in our predictions, we vary the unphysical parameter ξ as indicated above. These uncertainties are presented by upper and lower dashed lines. We find that our default predictions agree very well with recent NNLO results [18]. For example, when the Higgs boson mass is $m_H = 120\,\text{GeV}$, our calculations give $\sigma = 0.84\,\text{pb}$ at Tevatron and $\sigma = 35.9\,\text{pb}$ at LHC. However, the scale dependences are rather large. At LHC energy, it changes from about 20% when $m_H = 100\,\text{GeV}$ to about 50% when $m_H = 200\,\text{GeV}$. At Tevatron, it ranges from 40% to 50%, respectively. This fact indicates the necessity of the inclusion high-order corrections in the k_T-factorization formalism. But one should note that in the k_T-factorization the role of such a correction is very different in comparison with the corrections in the collinear approach, since part of the standard high-order corrections is already included at LO level in the k_T-factorization[5]. At the same time the theoretical uncertainties of the collinear QCD calculations, after inclusion of both NNLO corrections and soft-gluon resummation at the NNLL level, are about 10% in the low mass range $m_H < 200\,\text{GeV}$ [18].

[4] In contrast with the J2003 set 2 unintegrated gluons. See also the further discussion in the next section.

3.2 Higgs production in association with jets

Now we demonstrate how the k_T-factorization approach can be used to calculate the semi-inclusive Higgs production rates. The produced Higgs boson is accompanied by a number of gluons radiated in the course of the gluon evolution. As it has been noted in [38], on the average the gluon transverse momentum decreases from the hard interaction block towards the proton. As an approximation, we assume that the gluon k' closest to the Higgs compensates the whole transverse momentum of the virtual gluon participating in the gluon fusion, i.e. $\mathbf{k'}_T \simeq -\mathbf{k}_T$ (see Fig. 1). All the other emitted gluons are collected together in the proton remnant, which is assumed to carry only a negligible transverse momentum compared to $\mathbf{k'}_T$. This gluon gives rise to a final hadron jet with $\mathbf{p}_{\text{jet T}} = \mathbf{k'}_T$.

From the two hadron jets represented by the gluons from the upper and lower evolution ladder we choose the one carrying the largest transverse momentum, and then compute the Higgs with an associated jet cross section at the LHC energy. We have applied the usual cut on the final jet transverse momentum $|\mathbf{p}_{\text{jet T}}| > 20\,\text{GeV}$. Our predictions for the transverse momentum distribution of the Higgs + one jet production are shown in Fig. 7. As in the inclusive Higgs production case, we test four different m_H values in the transverse momentum ditributions. All curves here are the same as in Fig. 2. One can see the shift of the

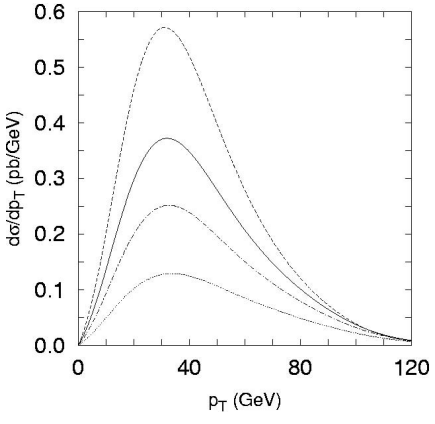

Fig. 7. Differential cross section $\mathrm{d}\sigma/\mathrm{d}p_T$ for Higgs boson + one jet production at $\sqrt{s} = 14\,\text{TeV}$. The kinematical cut $|\mathbf{p}_{\text{jet T}}| > 20\,\text{GeV}$ was applied. All curves are the same as in Fig. 2

[5] See [15, 34] for a more detailed discussion.

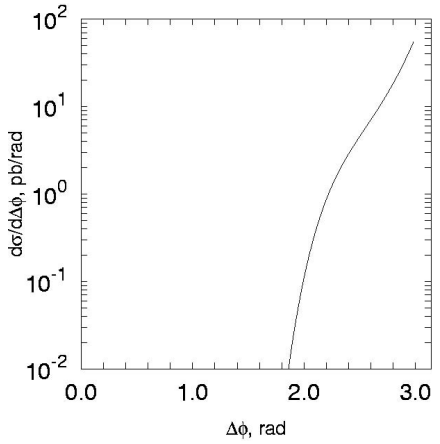

Fig. 8. The Higg–jet azimuthal angle distribution in the Higgs boson + one jet production at $\sqrt{s} = 14\,\text{TeV}$. The kinematical cut $|\mathbf{p}_{\text{jet T}}| > 20\,\text{GeV}$ was applied

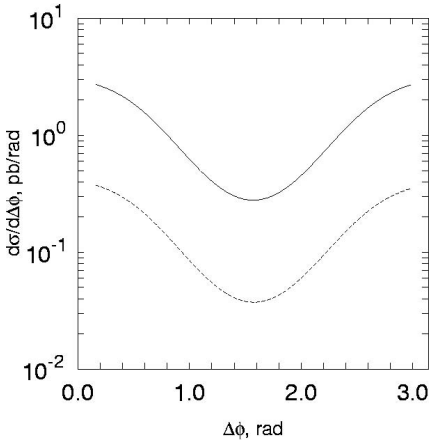

Fig. 9. The jet–jet azimuthal angle distribution in the Higgs boson + two jet production at $\sqrt{s} = 14\,\text{TeV}$. The kinematical cut $|\mathbf{p}_{\text{jet T}}| > 20\,\text{GeV}$ was applied for both jets. regel1000 Solid and dashed lines correspond to the J2003 set 1 and J2003 set 2 unintegrated gluon distributions, respectively

peak position in the p_T distributions in comparison with inclusive production, which is a direct consequence of the $|\mathbf{p}_{\text{jet T}}| > 20\,\text{GeV}$ cut. We note that the rapidity interval between the jet and the Higgs boson is naturally large. This is because there is angular ordering in the CCFM evolution, which is equivalent to an ordering in rapidity of the emitted gluons.

The investigation of the different azimuthal correlations between the final particles in semi-inclusive Higgs production provides many interesting insights. In particular, studying of these quantities is important to make a clean separation of the weak-boson fusion and gluon–gluon fusion contributions. To demonstrate the possibilities of the k_T-factorization approach, we present here the two azimuthal angle distributions. First, we calculate the azimuthal angle distribution between the Higgs boson and final jet transverse momenta in the Higgs + one jet production process. Second, we calculate the azimuthal angle distributions between the two final jet transverse momenta in the Higgs + two jet production process. In this case the Higgs boson is centrally located in rapidity between the two jets and it is very far from either jet, and the kinematical cut $|\mathbf{p}_{\text{jet T}}| > 20\,\text{GeV}$ was applied for both final jets. We set no cuts on the jet–jet invariant mass. Our results are shown in Figs. 8 and 9, respectively. Figure 8 demonstrates roughly the back-to-back Higgs + one jet production. In Fig. 9 we obtained a dip at 90 degrees in jet–jet azimuthal correlation, which is characteristic for a loop-induced Higgs coupling to gluons [39]. The deep origin at $\Delta\phi = \pi/2$ correlates with the presence of $\cos\phi_2$ in (6). In our approach, the k_T of the initial gluons is approximately compensated by the transverse momenta of the jets, and, consequently, $\Delta\phi \simeq \phi_2$. The fixed-order perturbative QCD calculations of the $gg \to ggH$ subprocess give the similar result [16]. However, as it was already mentioned above, such calculations are very cumbersome even at leading order. The evaluation of the radiative corrections at $\mathcal{O}(\alpha_s)$ to Higgs + two jet production would imply the calculation of up to hexagon quark loops and two-loop pentagon quark loops, which are at present unfeasible [20]. We note that the contribution from the weak-boson fusion to the Higgs + two jet production has a flat behavior of the jet–jet angular distribution [16, 20].

To illuminate the sensitivity of the Higgs production rates to the details of the unintegrated gluon distribution, we repeated our calculations for the jet–jet angular correlations using the J2003 set 2 gluon density [28] (dashed line in Fig. 9). This density takes into account the singular and non-singular terms in the CCFM splitting function, where the Sudakov and non-Sudakov form factors were modified accordingly. We note that the J2003 set 1 takes into account only singular terms. Both these sets describe the proton structure function $F_2(x, Q^2)$ at HERA reasonable well. However, one can see the very large discrepancy (about an order of magnitude) between the predictions of the J2003 set 1 and set 2 unintegrated gluon densities. A similar difference was claimed [28] for charm and bottom production at Tevatron also. This fact can be attributed to two possible reasons. First, the production of heavy Higgs boson is determined by the x values, which are in fact not small enough for applicability of the BFKL-like evolution. In addition to that, the BFKL and CCFM evolution equations include only the NLO contributions enhanced by the leading logarithms, while the "non-enhanced" next-order contributions are not taken into account. The fact that our predictions show a large sensitivity to the choice of the factorization scale can be taken as an indication that the non-leading logarithm contributions probably play an important role in our particular case.

4 Conclusions

We have considered the Higgs boson production via gluon–gluon fusion at high energy hadron colliders in the framework of the k_T-factorization approach. Our interests were focused on the Higgs boson total cross section and transverse momenta distributions at the Tevatron and LHC colliders. In our numerical calculations we use the J2003

set 1 unintegrated gluon distribution, which was obtained recently from the full CCFM evolution equation.

We find that k_T-factorization gives results very close to NNLO pQCD for the inclusive Higgs production total cross sections. This is because the main part of the high-order collinear pQCD corrections is already included in the k_T-factorization. Also we have demonstrated that k_T-factorization gives a possibility to investigate the associated Higgs boson and jets production in a much simpler manner than it can be done in the collinear factorization. Using some approximation, we have calculated the transverse momentum distributions and investigated the Higgs–jet and jet–jet azimuthal correlations in the Higgs + one or two jet production processes. However, the scale dependence of our calculations is rather large (of the order of 20–50%), which indicates the importance of the high-order correction within the k_T-factorization approach. These corrections should be developed and taken into account in future applications.

We point out that in this paper we do not try to give a better prediction for Higgs production than the fixed-order pQCD calculations. The main advantage of our approach is that it is possible to obtain in straighforward manner the analytic description which reproduces the main features of the collinear high-order pQCD calculations[6]. But in any case, the future experimental study of such processes at LHC will give important information about the non-collinear gluon evolution dynamics, which will be useful even for leading-order k_T-factorization formalism.

Acknowledgements. The authors are very grateful to H. Jung for the opportunity to use the CCFM code for the unintegrated gluon distributions in our calculations, for reading of the manuscript and useful discussion. We thank S.P. Baranov for encouraging interest and helpful discussions. N.Z. thanks P.F. Ermolov for support and the DESY directorate for hospitality and support. This research was supported in part by the FASI of Russian Federation (grant NS-1685-2003-2).

References

1. ATLAS Collaboration, Technical Design Report, Vol. 2, CERN/LHCC/99-15, 1999; CMS Collaboration, Technical Proposal, CERN/LHCC/94-38, 1994
2. F. Wilczek, Phys. Rev. Lett. **39**, 1304 (1977); H.M. Georgi, S.L. Glashow, M.E. Machacek, D.V. Nanopoulos, Phys. Rev. Lett. **40**, 692 (1978); J.R. Ellis, M.K. Gaillard, D.V. Nanopoulos, C.T. Sachrajda, Phys. Lett. B **83**, 339 (1979); T.G. Rizzo, Phys. Rev. D **22**, 178 (1980); D **22**, 1824 (1980)
3. D. Graudenz, M. Spira, P.M. Zervas, Phys. Rev. Lett. **70**, 1372 (1993); M. Spira, A. Djouadi, D. Graudenz, P.M. Zervas, Nucl. Phys. B **453**, 17 (1995)
4. N. Kauer, T. Plehn, D. Rainwater, D. Zeppenfeld, Phys. Lett. B **503**, 113 (2001); T. Plehn, D. Rainwater, D. Zeppenfeld, Phys. Rev. D **61**, 093005 (2000); D. Rainwater, D. Zeppenfeld, JHEP **9712**, 005 (1997)
5. V.N. Gribov, L.N. Lipatov, Yad. Fiz. **15**, 781 (1972); L.N. Lipatov, Sov. J. Nucl. Phys. **20**, 94 (1975); G. Altarelli, G. Parisi, Nucl. Phys. B **126**, 298 (1977); Y.L. Dokshitzer, Sov. Phys. JETP **46**, 641 (1977)
6. E.A. Kuraev, L.N. Lipatov, V.S. Fadin, Sov. Phys. JETP **44**, 443 (1976); **45**, 199 (1977); I.I. Balitsky, L.N. Lipatov, Sov. J. Nucl. Phys. **28**, 822 (1978)
7. V.N. Gribov, E.M. Levin, M.G. Ryskin, Phys. Rep. **100**, 1 (1983)
8. E.M. Levin, M.G. Ryskin, Yu.M. Shabelsky, A.G. Shuvaev, Sov. J. Nucl. Phys. **53**, 657 (1991)
9. S. Catani, M. Ciafoloni, F. Hautmann, Nucl. Phys. B **366**, 135 (1991)
10. J.C. Collins, R.K. Ellis, Nucl. Phys. B **360**, 3 (1991)
11. M. Ciafaloni, Nucl. Phys. B **296**, 49 (1988); S. Catani, F. Fiorani, G. Marchesini, Phys. Lett. B **234**, 339 (1990); Nucl. Phys. B **336**, 18 (1990); G. Marchesini, Nucl. Phys. B **445**, 49 (1995)
12. J.R. Forshaw, A. Sabio Vera, Phys. Lett. B **440**, 141 (1998)
13. B.R. Webber, Phys. Lett. B **444**, 81 (1998)
14. G.P. Salam, JHEP **03**, 009 (1999)
15. B. Andersson et al. (Small-x Collaboration), Eur. Phys. J. C **25**, 77 (2002)
16. V. Del Duca, W. Kilgore, C. Olear, C. Schmidt, D. Zeppenfeld, Nucl. Phys. B **616**, 367 (2001); Phys. Rev. D **67**, 073003 (2003)
17. J.R. Ellis, M.K. Gaillard, D.V. Nanopoulos, Nucl. Phys. B **106**, 292 (1976); M.A. Shifman, A.I. Vainstein, M.B. Voloshin, V.I. Zakharov, Yad. Fiz. **30**, 1368 (1979)
18. R.V. Harlander, W.B. Kilgore, Phys. Rev. Lett. **88**, 201801 (2002); C. Anastasiou, K. Melnikov, Nucl. Phys. B **646**, 220 (2002); V. Ravindran, J. Smith, W.L. van Neerven, Nucl. Phys. B **665**, 325 (2003)
19. S. Dawson, Nucl. Phys. B **359**, 283 (1991); A. Djouadi, M. Spira, P.M. Zervas, Phys. Lett. B **264**, 440 (1991)
20. V. Del Duca, hep-ph/0312184
21. J.C. Collins, D.E. Soper, Nucl. Phys. B **193**, 381 (1981); B **213**, 545 (1983); B **197**, 446 (1982)
22. J.C. Collins, D.E. Soper, G. Sterman, Nucl. Phys. B **250**, 199 (1985)
23. R.K. Ellis, S. Veseli, Nucl. Phys. B **511**, 649 (1998); R.K. Ellis, D.A. Ross, S. Veseli, Nucl. Phys. B **503**, 309 (1997)
24. S. Catani, E. D'Emilio, L. Trentadue, Phys. Lett. B **211**, 335 (1988); R.P. Kauffmann, Phys. Rev. D **45**, 1512 (1992)
25. D. de Florian, M. Grazzini, Phys. Rev. Lett. **85**, 4678 (2000); Nucl. Phys. B **616**, 247 (2001)
26. A. Gawron, J. Kwiecinski, Phys. Rev. D **70**, 014003 (2004)
27. M.G. Ryskin, A.G. Shuvaev, Y.M. Shabelski, Phys. Atom. Nucl. **64**, 120 (2001)
28. H. Jung, Mod. Phys. Lett. A **19**, 1 (2004)
29. G. Watt, A.D. Martin, M.G. Ryskin, Phys. Rev. D **70**, 014012 (2004), Erratum D **70**, 079902 (2004), hep-ph/0309096
30. B.R. Webber, Nucl. Phys. Proc. Suppl. C **18**, 38 (1991); G. Marchesini, B.R. Webber, Nucl. Phys. B **386**, 215 (1992); A. Gawron, J. Kwiecinski, Acta. Phys. Polon. B **34**, 133 (2003)
31. M.A. Kimber, A.D. Martin, M.G. Ryskin, Phys. Rev. D **63**, 114027 (2001)
32. H. Jung, Comput. Phys. Comm. **143**, 100 (2002)
33. F. Hautmann, Phys. Lett. B **535**, 159 (2002)
34. J. Andersen et al. (Small-x Collaboration), Eur. Phys. J. C **35**, 67 (2004)
35. G.P. Lepage, J. Comput. Phys. **27**, 192 (1978)

[6] In this part our conclusions coincide with the ones from [29].

36. A.V. Lipatov, N.P. Zotov, Eur. Phys. J. C **41**, 163 (2005)
37. S. Catani, D. de Florian, M. Grazzini, Nucl. Phys. B **596**, 299 (2001); JHEP **0201**, 015 (2002); G. Bozzi, S. Catani, D. de Florian, M. Grazzini, Phys. Lett. B **564**, 65 (2003); S. Catani, D. de Florian, M. Grazzini, P. Nason, JHEP **0307**, 028 (2003)
38. S.P. Baranov, N.P. Zotov, Phys. Lett. B **491**, 111 (2000)
39. T. Plehn, D. Rainwater, D. Zeppenfeld, Phys. Rev. Lett. **88**, 051801 (2002)